Cell Host & Microbe
Article

Amino Acid Starvation Induced by Invasive Bacterial Pathogens Triggers an Innate Host Defense Program

Ivan Tattoli,[1,2] Matthew T. Sorbara,[2] Dajana Vuckovic,[3] Arthur Ling,[1] Fraser Soares,[1] Leticia A.M. Carneiro,[4] Chloe Yang,[1] Andrew Emili,[3] Dana J. Philpott,[2] and Stephen E. Girardin[1,*]
[1]Department of Laboratory Medicine and Pathobiology
[2]Department of Immunology
[3]Department of Molecular Genetics
University of Toronto, Toronto, ON M6G 2T6, Canada
[4]Instituto de Microbiologia, Universidade Federal do Rio de Janeiro, Rio de Janeiro 21941-590, Brazil
*Correspondence: stephen.girardin@utoronto.ca
DOI 10.1016/j.chom.2012.04.012

SUMMARY

Autophagy, which targets cellular constituents for degradation, is normally inhibited in metabolically replete cells by the metabolic checkpoint kinase mTOR. Although autophagic degradation of invasive bacteria has emerged as a critical host defense mechanism, the signals that induce autophagy upon bacterial infection remain unclear. We find that infection of epithelial cells with *Shigella* and *Salmonella* triggers acute intracellular amino acid (AA) starvation due to host membrane damage. Pathogen-induced AA starvation caused downregulation of mTOR activity, resulting in the induction of autophagy. In *Salmonella*-infected cells, membrane integrity and cytosolic AA levels rapidly normalized, favoring mTOR reactivation at the surface of the *Salmonella*-containing vacuole and bacterial escape from autophagy. In addition, bacteria-induced AA starvation activated the GCN2 kinase, eukaryotic initiation factor 2α, and the transcription factor ATF3-dependent integrated stress response and transcriptional reprogramming. Thus, AA starvation induced by bacterial pathogens is sensed by the host to trigger protective innate immune and stress responses.

INTRODUCTION

Macroautophagy (herein termed autophagy) is a highly conserved cellular process through which cellular constituents such as dysfunctional organelles or macromolecular complexes are progressively engulfed into an isolation membrane. This results in the formation of a double-membrane structure that is targeted to lysosomes for degradation and recycling of its content. In conditions of nutrient or energy deprivation, autophagy is initiated, and this process represents a major pathway triggering nutrient recycling to sustain essential metabolic functions (Klionsky, 2007).

Autophagy induction is negatively controlled by the metabolic checkpoint kinase mTOR, which associates with the mTOR-interacting proteins Raptor and mLST8/GβL to form the core of the mTOR complex 1 (mTORC1) (Wullschleger et al., 2006). Besides negative regulation of autophagy, mTORC1 also controls central cellular functions, such as messenger RNA (mRNA) translation, cell growth, and ribosomal biogenesis, in part through the phosphorylation of S6K1 and 4EBP1 (Wullschleger et al., 2006). mTORC1 activity is under the tight control of cellular nutrient availability, and mTOR thus represents a central molecule linking nutrient sensing and basic cellular metabolic functions. Sensing of growth factors, oxygen tension and ATP levels all converge to stimulate the GTPase Rheb, which interacts with and activates mTORC1 at the surface of late endosomes/lysosomes (LE/Ly), where Rheb is constitutively located (Sengupta et al., 2010). Importantly, recent evidence demonstrated that the recruitment of mTORC1 to the surface of LE/Ly is dependent on intracellular amino acid (AA) availability (Sancak et al., 2008, 2010), thus providing a mechanistic explanation for why AA starvation can turn off mTORC1 signaling regardless of the availability of other mTORC1-activating metabolites. After sensing of intracellular AA pools by an unknown mechanism, Raptor is targeted to LE/Ly endomembranes through a pathway dependent on Rag GTPases and the trimeric Ragulator protein complex, composed of MP1, p14, and p18 (Sancak et al., 2010).

Invasion of host cells by bacterial pathogens triggers a number of innate immune responses, such as proinflammatory signaling and cell-autonomous restriction of bacterial growth. Among these host defense mechanisms, a critical role for autophagy-dependent targeting and degradation of intracellular bacteria was recently identified (Levine et al., 2011) and is termed xenophagy. In the past few years, important progress was made to elucidate how the autophagic machinery targets intracellular bacteria. Several pathways critical for the specific control of xenophagy have been identified, which depend on p62 (Yoshikawa et al., 2009), NDP52 (Thurston et al., 2009, 2012), Toll-like receptors (TLRs) (Xu et al., 2007), and Nod-like receptors (NLRs) (Cooney et al., 2010; Travassos et al., 2010). However, the identification of these pathways, although providing clues about how microbes are specifically targeted over other cellular constituents, does not explain how xenophagy is turned on in

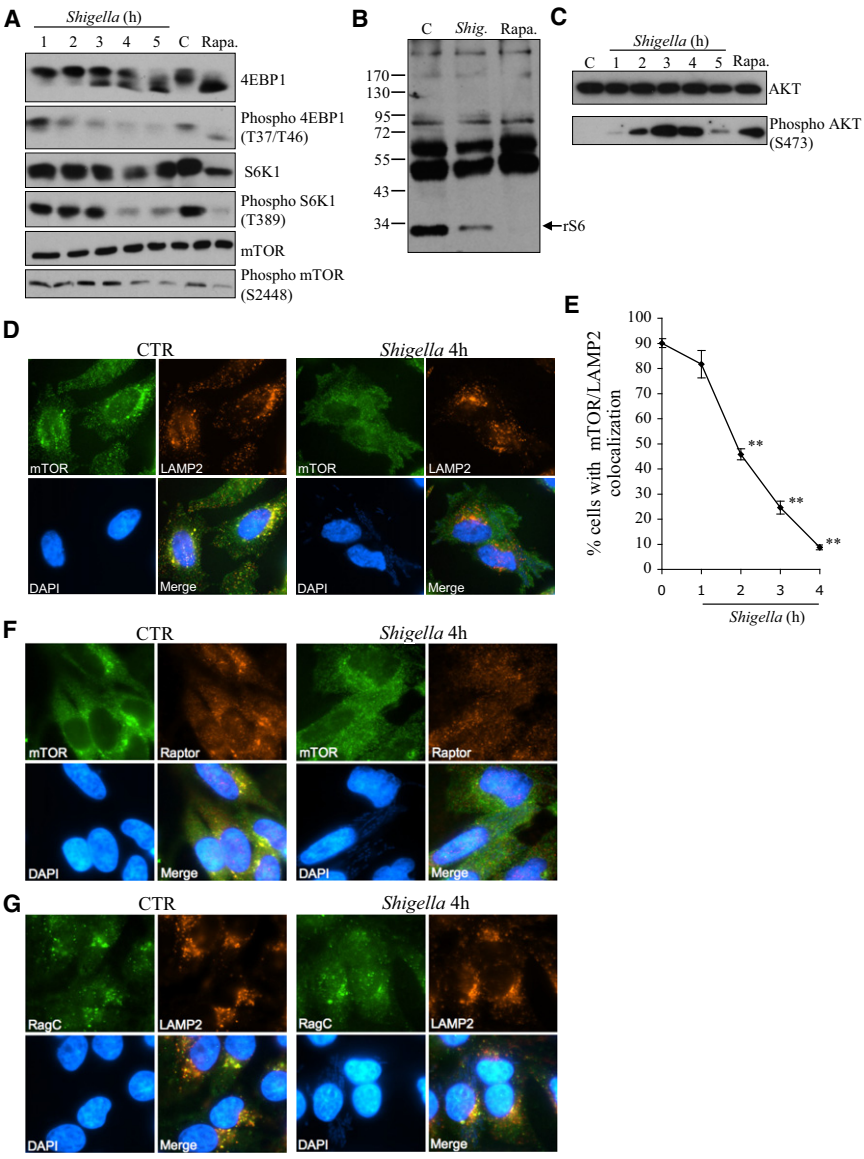

Figure 1. *Shigella* Induces mTORC1 Signaling Downregulation and Cytosolic Dispersion

(A) HeLa cells were infected with *Shigella* for 1 hr to 5 hr, or stimulated for 2 hr with rapamycin; lysates were analyzed by blotting with the indicated antibodies.

(B) HeLa cells were infected with *Shigella* for 4 hr or stimulated with rapamycin for 2 hr; lysates were analyzed by blotting with an antibody against AGC kinases substrates. S6 is the main protein migrating at approximately 30 kDa and detected by this antibody (Zhang et al., 2002).

(C) As in (A), but lysates were blotted with anti-AKT and anti-AKT phospho Ser473 antibodies.

(D) HeLa cells left unstimulated (CTR) or infected with *Shigella* for 4 hr, analyzed by IF with antibodies against mTOR and LAMP2.

(E) Percentage of *Shigella*-infected cells displaying mTOR localization to LAMP2+ vesicles. Values are means ± SEM. n = 3. **p < 0.01 over uninfected.

(F and G) HeLa cells left unstimulated (CTR) or infected 4 hr with *Shigella*, analyzed by IF with antibodies against mTOR and Raptor (F) or RagC and LAMP2 (G).

See also Figure S1.

the first place, given that this process is typically studied in metabolically replete cells. Indeed, it seems unlikely that xenophagy could represent an efficient host defense mechanism if constitutively suppressed by mTORC1. This led us to speculate that bacterial infection might affect cellular metabolism and mTOR signaling.

Here we show that bacterial infection triggered the rapid induction of an intracellular AA starvation state that, in the case of the cytoinvasive pathogen, *Shigella*, led to prolonged mTOR delocalization from LE/Ly endomembranes, inhibition of its activity, and induction of xenophagy. *Shigella*-induced AA starvation also triggered the activation of the GCN2/eIF2α signaling axis, leading to the accumulation of mRNA stress granules in the cytosol of infected cells, and ATF3-dependent reprogramming of the transcriptional response to the invasive pathogen. We further demonstrate that *Salmonella*, a pathogen that survives within modified endosomes, rapidly escaped these defense pathways, resulting in the recruitment and reactivation of mTOR at the surface of the *Salmonella*-containing vacuole (SCV) after replenishment of intracellular AA pools. Mechanistically, we showed that induction of AA starvation pathways in bacteria-infected cells was caused by membrane damage. Finally, we demonstrated that the downregulation of AA starvation-dependent pathways allowed *Salmonella* to escape degradation mediated by autophagy. These results reveal the critical role played by AA starvation and mTOR signaling in the host response to intracellular bacterial pathogens, and demonstrate how *Salmonella* controls both AA starvation pathways and mTOR cellular trafficking to downregulate host innate immune defenses.

RESULTS

Shigella Infection Inhibits mTOR Activity and Endomembrane Targeting

Although mTOR signaling controls numerous cellular processes, including autophagy, the impact of bacterial infection on mTOR-dependent signaling remains poorly understood. To gain insights into this question, we infected HeLa cells with *Shigella*, a Gram-negative bacterial pathogen that invades host cells, rapidly ruptures the endocytic vacuole, and is found free in the host cytosol. Strikingly, infection resulted in a strong and sustained downregulation of the phosphorylation of S6K1 and 4EBP1, two major targets of mTOR (Figure 1A). Moreover, both *Shigella* infection and rapamycin stimulation potently reduced the phosphorylation of S6, a major S6K1 target (Figure 1B).

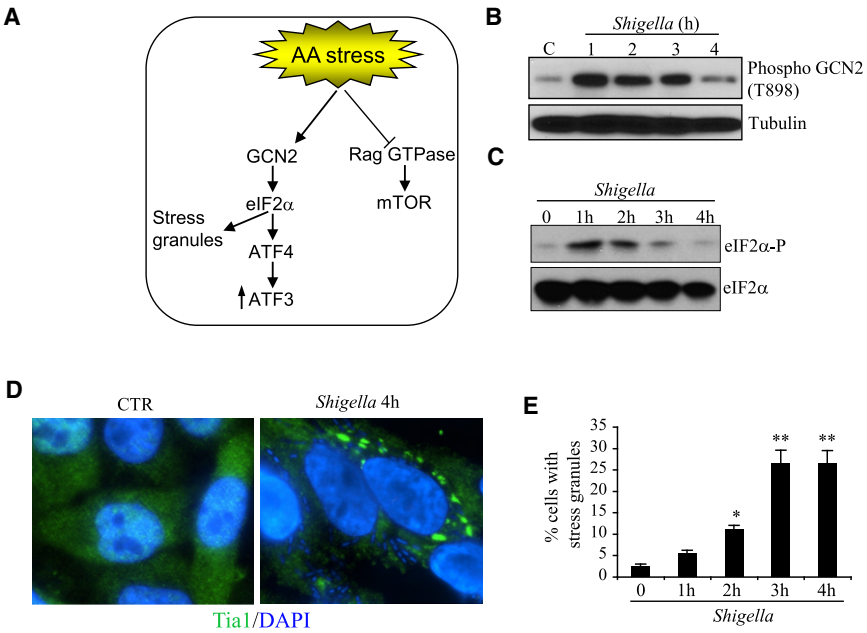

Figure 2. *Shigella* Infection Triggers AA Starvation

(A) Key aspects of the AA stress response program in mammalian cells.

(B and C) HeLa cells infected with *Shigella* for 1 hr to 4 hr, analyzed by blotting with anti-Phospho GCN2 (T898) and anti-tubulin antibodies (B) or anti-Phospho eIF2α (S51) and anti-eIF2α antibodies (C).

(D) HeLa cells left unstimulated (CTR) or infected with *Shigella* for 4 hr, analyzed by IF with anti-Tia-1 antibody, while host nuclei and bacteria are visualized with DAPI.

(E) Percentage of *Shigella*-infected cells displaying Tia-1+ stress granules. Values are means + SEM. n = 3.

(F) Mouse embryonic fibroblasts (MEFs) from wild-type (WT) and eIF2α S51A knockin (KI) mice infected 4 hr with *Shigella*, analyzed by IF as in (D).

(G) Free L-leucine and L-isoleucine concentration in lysates from unstimulated cells (CTR), cells incubated 4 hr in Krebs-Ringer Buffer (KRB) or infected with *Shigella* for 1 to 4 hr. Values are means + SD of six replicates from two independent experiments.

AKT is a critical upstream regulator of mTORC1, and AKT phosphorylation reflects activation. Moreover, mTORC1 inhibition by rapamycin induces AKT phosphorylation, thereby providing a crucial feedback loop on mTOR signaling (Huang and Manning, 2009). We observed that *Shigella* infection resulted in a strong induction of AKT phosphorylation on Ser473, which peaked at 3–4 hr post-infection (p.i.) (Figure 1C). This result likely reflects the progressive downregulation of mTORC1 signaling in *Shigella*-infected cells and shows that *Shigella*-mediated inhibition of mTORC1 signaling occurs at a step downstream of AKT.

We next used immunofluorescence (IF) to track the subcellular distribution of endogenous mTOR after infection. mTOR localized to LAMP2+ LE/Ly compartments in noninfected cells (Figure 1D), as previously reported (Sancak et al., 2008). Interestingly, *Shigella* infection resulted in a rapid and sustained cytosolic relocalization of mTOR in infected cells (Figures 1D–1E). In contrast, the mTORC1 inhibitor rapamycin (Figure S1A available online) and an AKT inhibitor (Figure S1B) failed to induce cytosolic redistribution of mTOR, thus showing that mTORC1 pathway inhibition is not the cause of mTOR subcellular redistribution.

mTOR localization to LE/Ly first requires targeting of Raptor to a complex composed of Rag GTPases and the Ragulator, which constitutively localizes to the surface of LE (Sancak et al., 2008, 2010). Interestingly, *Shigella* infection resulted in cytosolic dispersion of Raptor staining (Figure 1F) while RagC still colocalized with LAMP2+ compartments (Figure 1G), suggesting that infection inhibited mTOR signaling at the level of Raptor targeting to the Rag/Ragulator complex. Next, a constitutively active form of RagB GTPase rescued mTOR LE/Ly localization in *Shigella*-infected cells (Figure S1C), thus showing that impaired recruitment of Raptor/mTOR to Rag GTPases was caused by decreased activity of Rag GTPases. Similarly, overexpression of a Raptor construct engineered to localize constitutively to LE/Ly membranes by bypassing the action of Rag GTPases, was sufficient to target mTOR to LE/Ly membranes in *Shigella*-infected cells (Figure S1D). Together, these results show that *Shigella* infection downregulates mTORC1 activity by displacing mTOR from LAMP2+ LE/Ly vesicles, at the level of Raptor targeting to Rag GTPases (Figure S1E).

Shigella Infection Induces a General AA Starvation Response

Recent evidence demonstrated that AA sufficiency is the physiological cue that allows targeting of mTOR/Raptor to Rag/Ragulator, at the surface of LE/Ly (Sancak et al., 2010) (Figure 2A). The results above prompted us to determine whether *Shigella* infection triggered a general state of cytosolic AA starvation despite the fact that infection was performed in an AA-rich medium. In support for this, the intracellular AA sensor GCN2 was rapidly phosphorylated in *Shigella*-infected cells, indicating acute AA starvation (Figure 2B), and so was also the GCN2 target eIF2α (Figure 2C), which controls a key step in mRNA translation during cellular stress (Wek et al., 2006). Furthermore, induction of the GCN2/eIF2α axis after *Shigella* infection resulted in the formation of Tia-1-rich mRNA stress granules (Figures 2D and 2E), which

were dependent on eIF2α phosphorylation, as evidenced by the fact that stress granules did not form in mouse embryonic fibroblasts carrying the knockin S51A eIF2α mutation (Figure 2F).

In order to demonstrate directly that *Shigella* infection induced an acute phase of intracellular AA starvation despite the presence of excess AA concentrations in the extracellular milieu, we used liquid chromatography/mass spectrometry (LC/MS) to analyze by LC-MS/MS the cytosolic concentration of free L-leucine and L-isoleucine, two AAs whose intracellular levels play key roles in controlling mTOR (Avruch et al., 2009). Importantly, *Shigella* infection resulted in a rapid and sustained reduction of cytosolic L-leucine/L-isoleucine levels (Figure 2G), although the effect was not as profound as when cells were incubated for 4 hr in AA-starvation Krebs-Ringer Buffer (KRB).

Therefore, our results establish that *Shigella* infection induces a general state of AA starvation that, in turn, triggers GCN2/eIF2α-dependent stress response pathway and mRNA stress granule formation.

Key Role of ATF3 in the Transcriptional Reprogramming of *Shigella*-Infected Cells

Having established that *Shigella* triggers a general AA starvation state in infected cells, we aimed to identify, at a genome-wide scale, the transcriptional impact of mTOR inhibition in *Shigella*-infected cells. To do so, RNAs collected from unstimulated, *Shigella*-infected or rapamycin-stimulated HeLa cells were hybridized on Affymetrix microchips. As expected, we first observed that *Shigella* infection resulted in the upregulation of numerous genes associated with inflammation (such as *IL-8*, *CXCL10*, *PTX3*, and *IL-32*) and NF-κB signaling (including *TNFAIP3/A20* and *NFKB1A*), which were not induced in rapamycin-stimulated cells (Figure S2).

We next noticed that a large group of 87 genes were jointly upregulated in both *Shigella*-infected cells (n = 316 genes upregulated over 1.5-fold) and rapamycin-stimulated cells (n = 430 genes upregulated over 1.5-fold), thus showing the existence of a highly significant ($p = 5.26 \times 10^{-30}$) common transcriptional signature for these two conditions. These 87 common hits were further classified based on their relative fold induction ranking in *Shigella*-infected and rapamycin-stimulated cells (Figures 3A and S2), which revealed the critical importance of the ATF3-dependent pathway as a signaling circuit common to *Shigella*-infected and mTOR-inhibited cells. Indeed, two genes of this pathway, the transcription factor *ATF3* itself and the ATF3 target *CHAC1*, were among the ten most upregulated genes in both conditions, while four documented (*PMAIP1/NOXA*, *CHOP/DDIT3*, *KLF6*, and *GADD45G*) and three predicted (*JUN*, *WFDC3*, and *GABARAPL1/ATG8*) ATF3 target genes were also found in the group of 87 genes induced over 1.5-fold by *Shigella* and rapamycin. These results were validated by quantitative PCR (qPCR) for *ATF3*, *CHAC1*, and *CHOP* (Figures 3B–3D), as well as for *GGT1*, *IFITM5*, *JUN*, and *KLF6* (data not shown). As expected, ATF3, CHAC1, and CHOP were also strongly induced by AA starvation (Figures 3E–3G). Finally, kinetic analyses showed that while *ATF3* was induced as early as 1 hr p.i. and its expression remained high at 4 hr p.i., the expression of the ATF3 target *CHAC1* increased steadily over time in *Shigella*-infected cells (Figures 3H–3J). Of note, our results clearly show that mTOR inhibition by rapamycin directly triggers ATF3-dependent signaling, although the pathway involved remain uncharacterized, which also implies that *Shigella*-induced ATF3 activation likely results from the concomitant induction of the well-characterized GCN2/eIF2α/ATF4/ATF3 integrated stress response (ISR) (Jiang et al., 2004) and the inhibition of mTOR.

Together, these results demonstrate that, in addition to the well-characterized proinflammatory response, intracellular *Shigella* induces an acute host transcriptional reprogramming correlating with mTOR downregulation and geared toward stress-associated ATF3 signaling.

Manipulation of mTOR Signaling and Localization by *Salmonella*

In order to determine if the above observations were a general characteristic of cellular invasion by bacterial pathogens, we next infected HeLa cells with *Salmonella* Typhimurium, a Gram-negative bacterial pathogen that progressively remodels the SCV in order to establish an intracellular replicative niche (Ramsden et al., 2007). Similar to *Shigella* infection, *Salmonella* infection resulted in decreased phosphorylation of 4EBP1 (Figure 4A). Unexpectedly, S6K1 phosphorylation did not follow this trend, as the protein was even hyperphosphorylated (Figure 4A). This observation was supported by the fact that ribosomal S6 protein phosphorylation was not downregulated by *Salmonella* infection (Figure 4B). Because 4EBP1 and S6K1 phosphorylation normally follow similar profiles, these results suggest the existence of a *Salmonella*-specific mechanism of mTOR signaling manipulation.

We speculated that specific effectors delivered by *Salmonella* could account for the manipulation of mTOR signaling that we observed. The *Salmonella* pathogenicity island 1 (SPI-1) effector SopB is rapidly injected into host cells, resulting in hyperactivation of AKT (Steele-Mortimer et al., 2000). Interestingly, *Salmonella*-induced S6K1 hyperphosphorylation appeared to depend, in the first hour p.i., on SopB (Figure 4C), which activated AKT with the same kinetics (Figure S3A), as previously shown (Steele-Mortimer et al., 2000). However, at later time points, S6K1 hyperphosphorylation was SopB-independent (Figure 4C), suggesting that other mechanisms account for S6K1 sustained phosphorylation at later times of infection. Of note, S6K1 hyperphosphorylation remained rapamycin sensitive (Figure S3B).

We next followed mTOR cellular localization in *Salmonella*-infected cells. In the first 2 hr of infection, mTOR localization to LAMP2+ LE/Ly compartments was severely blunted overall (Figures 4D and 4E), and this correlated with the rapid activation of GCN2 (Figure 4F), decrease in cytosolic levels of free L-leucine and L-isoleucine (Figure 4G), the transcriptional induction of *ATF3*, *CHAC1*, and *CHOP* (Figures 4H and S3C) and the accumulation of mRNA stress granules (data not shown), as early as 1 hr p.i. Therefore, similar to *Shigella*, *Salmonella* infection induced a rapid state of cytosolic AA starvation.

In a second phase of the infection, we were surprised to notice that mTOR was found to progressively relocalize to maturing SCVs (Figures 4D and 4E), an event that could be observed as early as 1 hr p.i., but was dramatically amplified starting at 3 hr p.i. mTOR relocalization to the SCV was not significantly altered in SopB-*Salmonella* (Figure S3D), thus showing that the

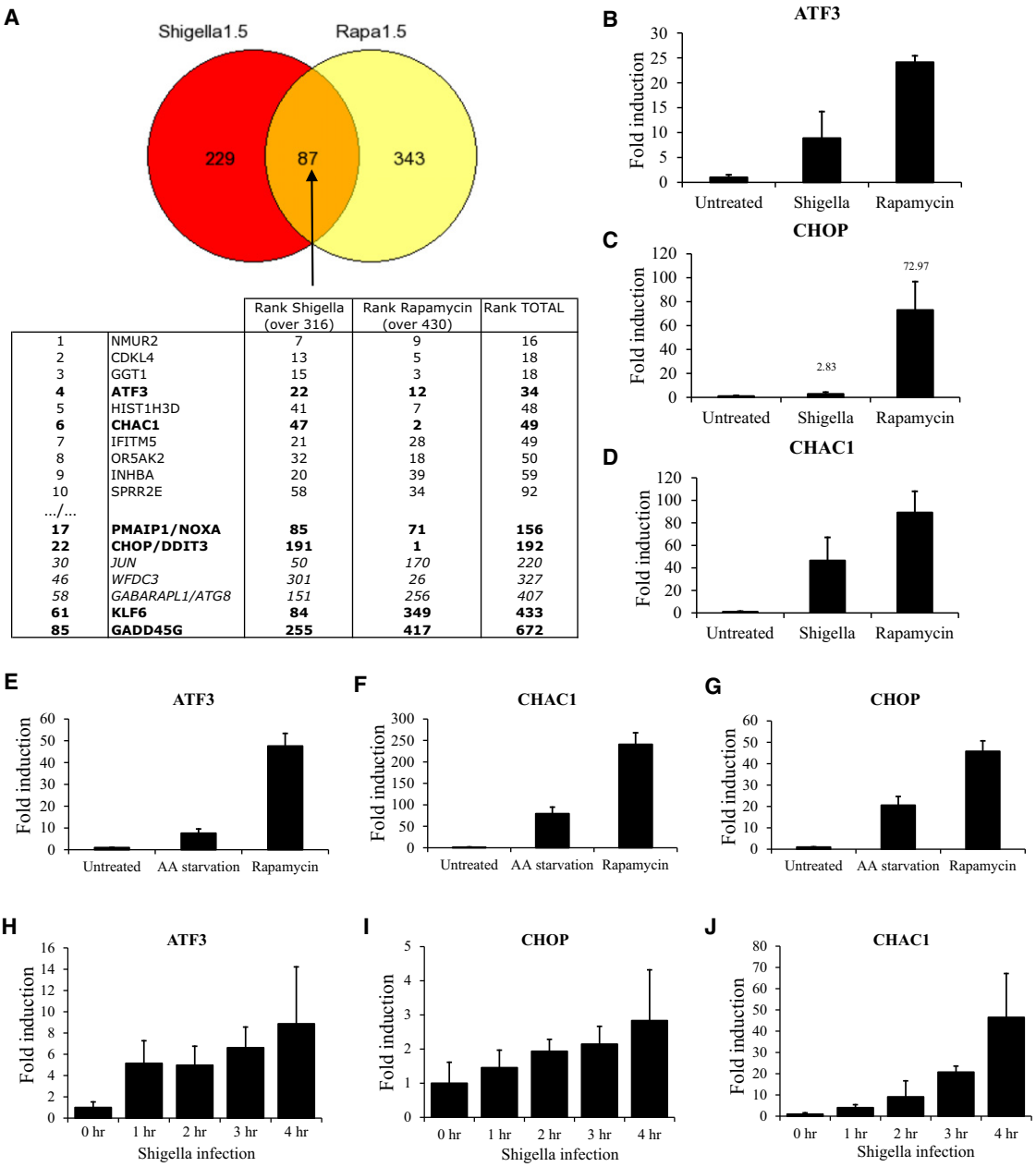

		Rank Shigella (over 316)	Rank Rapamycin (over 430)	Rank TOTAL
1	NMUR2	7	9	16
2	CDKL4	13	5	18
3	GGT1	15	3	18
4	**ATF3**	**22**	**12**	**34**
5	HIST1H3D	41	7	48
6	**CHAC1**	**47**	**2**	**49**
7	IFITM5	21	28	49
8	OR5AK2	32	18	50
9	INHBA	20	39	59
10	SPRR2E	58	34	92
.../...				
17	**PMAIP1/NOXA**	**85**	**71**	**156**
22	**CHOP/DDIT3**	**191**	**1**	**192**
30	*JUN*	*50*	*170*	*220*
46	*WFDC3*	*301*	*26*	*327*
58	*GABARAPL1/ATG8*	*151*	*256*	*407*
61	**KLF6**	**84**	**349**	**433**
85	**GADD45G**	**255**	**417**	**672**

Figure 3. ATF3-Dependent Transcriptional Reprogramming in *Shigella*-Infected Cells

(A) Top: Venn diagram from microarray analysis of HeLa cells infected with *Shigella* or stimulated with rapamycin for 4 hr, and displaying the number of genes induced over 1.5-fold. Bottom: Genes induced by both conditions were further ranked by addition of induction rankings for individual conditions. Genes in bold are known ATF3 target genes, and those in italics are predicted (from the Nextbio database).

(B–D) qPCR analysis of *ATF3* (B), *CHOP* (C), and *CHAC1* (D) induction after 4 hr *Shigella* infection or 4 hr rapamycin stimulation. Values are means + SEM. n = 3.

(E–G) qPCR analysis of *ATF3* (E), *CHOP* (F), and *CHAC1* (G) induction after 4 hr KRB or rapamycin stimulation. Values are means + SEM. n = 3.

(H–J) qPCR analysis of *ATF3* (H), *CHOP* (I), and *CHAC1* (J) induction after infection with *Shigella* for 1 to 4 hr. Values are means + SEM. n = 3.

See also Figure S2.

normalization of AKT phosphorylation was not the cause for the changes in mTOR subcellular localization. Concomitantly, and in contrast with *Shigella* infection, *Salmonella* infection resulted in a progressive normalization of cytosolic levels of L-leucine and L-isoleucine (Figure 4G), downregulation of *ATF3* expression (Figure 4H), and a disappearance of mRNA stress granules (data not shown), thus showing that *Salmonella*-induced AA starvation was transient. Together, these results demonstrate that *Salmonella* infection triggered a transient AA starvation response and suggest that a *Salmonella*-triggered mTOR complex, permissive to S6K1 but not 4EBP1 activation, is formed at the surface of the maturing SCV, at times of cytosolic AA normalization.

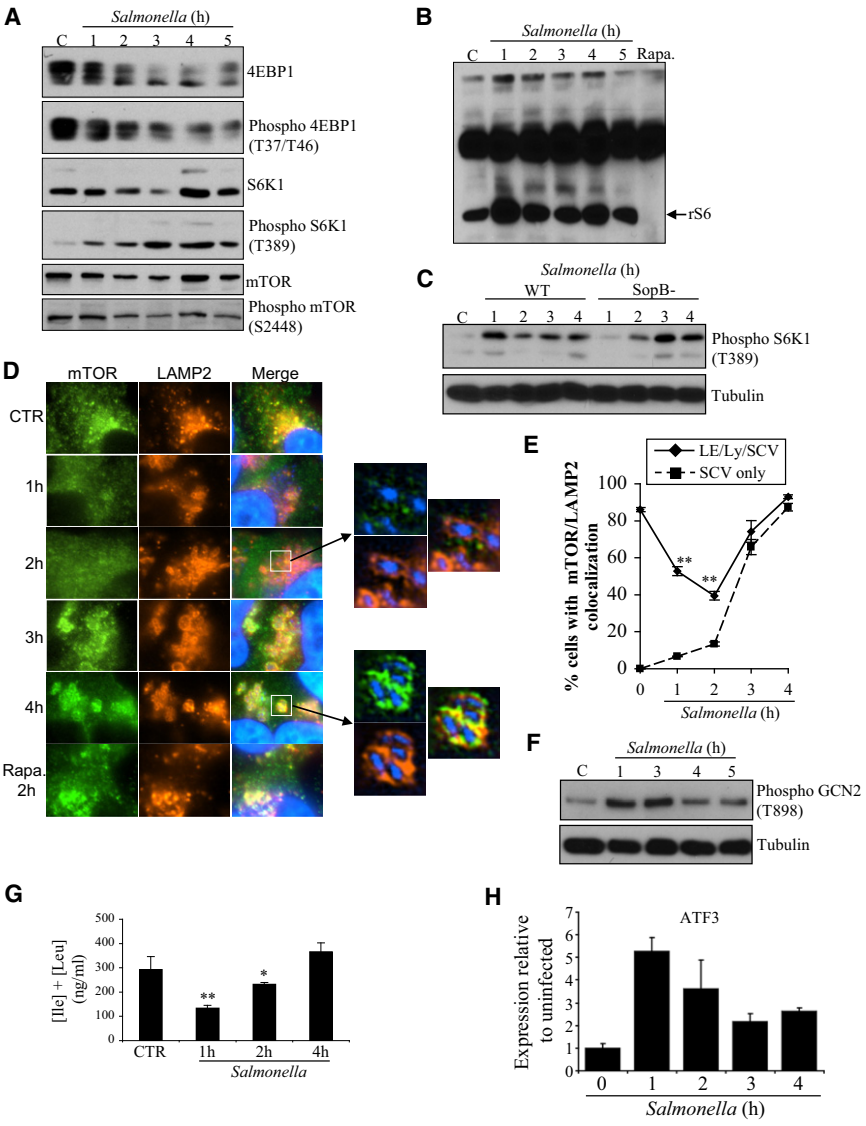

Figure 4. *Salmonella* Modulates mTORC1 Signaling

(A and B) HeLa cells infected with *Salmonella* for 1 to 5 hr analyzed by blotting with the antibodies indicated.

(C) HeLa cells infected with wild-type (WT) or SopB– *Salmonella* strains, analyzed by blotting with the antibodies indicated.

(D) HeLa cells left unstimulated (CTR), infected with *Salmonella* for 1 to 4 hr, or stimulated 2 hr with rapamycin, analyzed by IF with antibodies against mTOR and LAMP2. DAPI was used to visualize nuclei and bacteria.

(E) Percentage of *Salmonella*-infected cells displaying mTOR localization to LAMP2+ vesicles. Values are means ± SEM. n = 3.

(F) HeLa cells infected with *Salmonella* for 1 to 4 hr analyzed by blotting with anti-Phospho GCN2 (T898) and anti-tubulin antibodies.

(G) Free L-leucine and L-isoleucine concentration in lysates from cells either uninfected (CTR) or infected for 1 to 4 hr with *Salmonella*. Values are means + SD of six replicates from two independent experiments.

(H) qPCR analysis of *ATF3* induction in HeLa cells infected with *Salmonella*. Values are means + SEM. n = 3. *p < 0.05, **p < 0.01 over uninfected. See also Figure S3.

knockdown of RagB, RagC, or the Ragulator protein p18 all resulted in blunted mTOR targeting to SCVs and S6K1 activation (Figures 5E and 5F). It must be noted, however, that knockdown of Rag GTPases or the Ragulator also resulted in partial degradation of S6K1 in *Salmonella*-infected cells, which further amplified the observed decrease in S6K1 phosphorylation (Figure 5F). Finally, we observed by IF that RagC efficiently accumulated to the SCV already at 2 hr p.i. (Figure S4B). This supports the notion that mTOR/Raptor failure to localize to the SCV in the first hours of infection (1–2 hr p.i.; see Figure 4) resulted from cytosolic AA starvation rather than inefficient recruitment of the Ragulator/Rag complex.

Localization of mTOR to the SCV Requires AA and the Raptor/Rag/Ragulator Pathway

Because the SCV is a unique compartment previously unrecognized to host mTOR complexes, we aimed to characterize the mechanism underlying mTOR relocalization to these vesicles. By comparing infection performed for 4 hr either in normal DMEM or AA-starvation KRB medium, we first observed that both mTOR targeting to SCVs and S6K1 activation were fully dependent on the presence of AA (Figures 5A and 5B), in agreement with the above results (see Figure 4) that showed a temporal correlation between cytosolic AA replenishment and mTOR targeting to SCVs.

Using lentiviral-mediated RNA interference, we next observed that mTOR localization to SCVs, as well as S6K1 induction, were Raptor dependent and Rictor independent (Figures 5C and 5D). Accordingly, the kinetics of Raptor localization to SCVs closely matched those for mTOR, with cytosolic dispersion occurring at 2 hr p.i., followed by accumulation on the SCVs at 4 hr p.i. (Figure S4A). Further, short hairpin RNA (shRNA)-mediated

Rheb is anchored to the lysosomal membrane and is required for mTORC1 activation. Because *Salmonella* has evolved virulence strategies to limit fusion of the SCVs with lysosomes (Brumell and Grinstein, 2004), we investigated whether Rheb was required for mTOR reactivation after *Salmonella* infection. Importantly, while knockdown of Rheb expression did not affect the overall recruitment of mTOR to SCVs (Figure S4C), it dramatically reduced S6K1 activation, both in the early (1 hr p.i.) SopB-dependent phase, and at a late stage (4 hr p.i.) of *Salmonella* infection (Figure S4D).

Together, these results establish the critical importance of the Raptor/Rag GTPase/Ragulator axis, triggered by intracellular AA levels, in the reactivation of mTOR at the SCV (see also Figure S4E).

Membrane Damage Causes Intracellular AA Starvation

We next aimed to identify the mechanism responsible for the acute intracellular AA starvation observed in bacteria-infected cells, which caused mTOR inhibition and GCN2/ATF3 induction. We first speculated that host AA could be actively consumed by intracellular bacteria for their protein metabolism. However, specific inhibition of bacterial protein synthesis by the antibiotic chloramphenicol did not significantly affect *ATF3* upregulation in *Salmonella*-infected cells (Figure 6A), suggesting that induction of the AA starvation response was a host-driven mechanism triggered by bacterial invasion. In order to identify whether specific bacterial products presented to the host cytosol during infection were required for AA starvation responses, we used a procedure through which bacterial supernatants reach the host cytosol in cells transiently permeabilized with digitonin. Cytosolic presentation of *Shigella* supernatant was required to trigger IL-8 expression (Figure 6B), and we previously demonstrated that this occurred through the activation of Nod1-dependent NF-κB signaling in digitonin-permeabilized epithelial cells (Girardin et al., 2003). Surprisingly, we observed that digitonin-mediated membrane permeabilization, in the absence of bacterial supernatant, was sufficient to induce very robust *ATF3* expression (Figure 6C), as well as phosphorylation of GCN2 (Figure 6D). These results suggest that aseptic membrane damage acts as a danger signal that activates the GCN2/ATF3-dependent AA starvation pathway. It was recently shown that Galectin-8 and NDP52 are rapidly recruited to damaged host membranes (Thurston et al., 2012). In support for the notion that digitonin causes a membrane damage signal, NDP52 accumulated at discrete intracellular large foci in digitonin-permeabilized cells (Figure 6E). NDP52 recruitment was only transient, however, suggesting that membrane repair likely accounted for the normalization of the subcellular localization of NDP52. Although digitonin triggered a GCN2/ATF3-dependent pathway of AA starvation signaling, the drug did not alter mTOR localization to LE/Ly (Figure S5A), reflecting the fact that digitonin is thought to affect mainly the plasma membrane. In contrast, Glycyl-L-phenylalanine 2-naphthylamide (GPN), an endocytosed molecule that causes lysosomal membrane damage, induced the rapid accumulation of NDP52 to LAMP2+ LE/Ly (Figure S5B), GCN2 phosphorylation (Figure S5C), and mTOR dissociation from LE/Ly membranes (Figure S5D). Therefore, aseptic damage to host plasma membrane or lysosomes was sufficient to trigger AA starvation pathways, but only lysosomal damage resulted in mTOR inhibition, arguing for a potential compartmentalization of these responses.

We next aimed to determine whether membrane damage could account for the induction of AA starvation in bacteria-infected cells. Using NDP52 accumulation as a dynamic marker of host membrane damage, we observed that NDP52 was recruited to intracellular *Salmonella* at 1–2 hr p.i. as previously described (Cemma et al., 2011; Thurston et al., 2009), which was followed by a complete normalization of NDP52 staining by 4 hr p.i (Figures 6F and 6G). This shows that the transient induction of AA starvation in *Salmonella*-infected cells is caused by a brief event of SCV membrane damage occurring at approximatly 1–2 hr p.i. In contrast, NDP52 accumulation to intracellular membranes in *Shigella*-infected cells persisted up to 4 hr p.i. (Figures 6H and 6I), suggesting that sustained AA starvation in *Shigella*-infected cells was caused by long-lasting damage to host endomembranes through a yet uncharacterized mechanism.

Together, these results identify a critical link between host membrane damage caused by intracellular bacterial pathogens and AA starvation responses. These observations further suggest that the normalization of intracellular AA pools in *Salmonella*-infected cells at late stages of infection (3–4 hr p.i.) is explained by the transient nature of the membrane damage caused by this bacterium.

Reactivation of mTOR by *Salmonella* Results in Autophagy Escape

We speculated that a major consequence of mTORC1 modulation after bacterial infection would be the regulation of xenophagy. In support of the above hypothesis, the number of bacterial autophagosomes counted in infected cells inversely mirrored results obtained above for mTOR localization to endomembranes. Indeed, the number of LC3+ *Shigella* autophagosomes steadily increased over time, while *Salmonella* was targeted to autophagosomes at 1 and 2 hr p.i., and much less at later times points (Figure 7A), in agreement with previous reports (Birmingham et al., 2006; Ogawa et al., 2005; Travassos et al., 2010). These results suggest that pathogenic reactivation of mTOR in *Salmonella*-infected cells might confer an advantage to the bacteria by inhibiting autophagy induction, thereby limiting growth restriction. To test this hypothesis, cells were infected with *Salmonella* in the presence or absence of rapamycin, in order to determine whether autophagy induction by this drug could overcome the capacity of *Salmonella* to avoid autophagy-mediated clearance. Increased numbers of bacteria (1.6- to 2.6-fold more) were recovered in vehicle-stimulated over rapamycin-stimulated cells (Figure 7B). In contrast, rapamycin had no overall effect on *Shigella* growth restriction (Figure 7B), in agreement with our observation that this pathogen already effectively downregulates mTORC1 activity. We next confirmed that rapamycin-mediated restriction of *Salmonella* growth indeed required autophagy, since this effect was abolished in ATG16L1 knockdown cells (Figure 7C). In order to investigate whether the poor and transient targeting of *Salmonella* by autophagy (see Figure 7A) was solely a consequence of mTOR reactivation, or had other additional causes, recruitment of the autophagy marker GFP-LC3 to intracellular *Salmonella* was followed in vehicle-stimulated and rapamycin-stimulated cells. Rapamycin stimulation resulted in a dramatic increase of LC3-targeted *Salmonella*, (Figures 7D and 7E), thus showing that mTOR reactivation is the primary cause of *Salmonella*-dependent escape from autophagy. Finally, autophagic targeting of *Salmonella* at late time points (4 hr p.i.) was strongly increased in cells knocked down for the expression of the Ragulator protein p18 (Figure 7F). This shows that mTOR reactivation following normalization of cytosolic AA levels in *Salmonella*-infected cells accounts for the reduced autophagic targeting of *Salmonella* in the later phase of infection (3–4 hr p.i.).

DISCUSSION

Bacterial infection triggers a wide spectrum of host innate immune signaling pathways, such as those dependent on NF-κB, MAP kinase, or the caspase-1 inflammasome. Here we

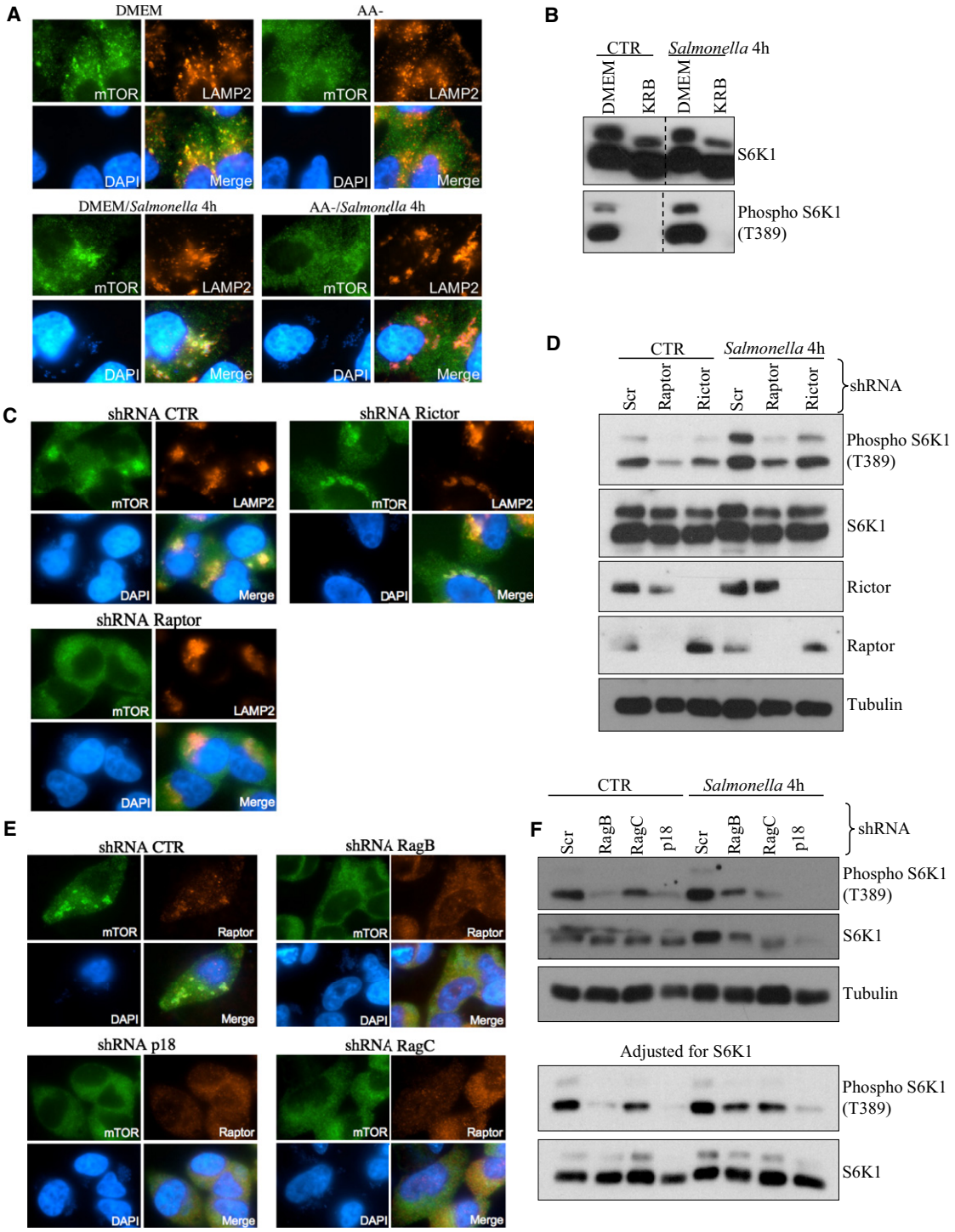

Figure 5. mTOR Relocalization to the SCV Depends on AA Uptake and the Raptor/Rag/Ragulator Pathway

(A) HeLa cells left uninfected or infected with *Salmonella* for 4 hr in DMEM or AA starvation medium KRB (AA–) analyzed by IF with antibodies against mTOR and LAMP2.

(B) HeLa cells left uninfected or infected with *Salmonella* for 4 hr in DMEM or KRB analyzed by blotting with the antibodies indicated.

(C) HeLa cells transduced with lentiviral particles targeting a scramble sequence (shRNA CTR), Rictor, or Raptor infected with *Salmonella* for 4 hr, analyzed by IF as in (A).

(D) HeLa cells transduced with lentiviral particles targeting a scramble sequence (Scr), Rictor, or Raptor left uninfected or infected with *Salmonella* for 4 hr, analyzed by blotting with the antibodies indicated.

(E) HeLa cells transduced with lentiviral particles targeting a scramble sequence (shRNA CTR), RagB, RagC, or Ragulator p18 infected with *Salmonella* for 4 hr, analyzed by IF as in (A).

provide evidence that intracellular AA starvation is a previously unrecognized critical arm of the host response to invasive bacteria, which modulates several cellular pathways (mTOR and GCN2/eIF2α) and processes (ISR induction, stress granule accumulation, autophagy induction). Our results also identify membrane damage as the upstream signal that triggers AA starvation in bacteria-infected cells. We also demonstrate that a bacterial pathogen (*Salmonella*) can promote the assembly of the mTOR-activating platform on modified host vesicles (the SCVs), resulting in efficient escape from autophagy-mediated degradation.

The AA starvation response, TOR pathway, and autophagy are highly conserved signaling modules, which regulate essential metabolic circuits and stress responses to the environment, from yeast to mammals. Our results imply that these signaling circuits may thus represent some of the most ancient innate defense mechanisms against invading bacterial pathogens, predating in evolution other innate immune regulatory networks, such as those that implicate TLRs, NLRs, or even NF-κB. This suggests that host responses to invasive pathogens might have evolved from primordial general metabolic stress responses.

Our results call for a reinterpretation of studies on xenophagy that claim the existence of bacteria-driven mechanisms of autophagy escape. We propose that efficient subversion can occur either by counteracting detection by the autophagy system (the current view) or by favoring the normalization of metabolic stress, as observed here in the case of *Salmonella* infection. In this context, it is interesting to speculate that *Shigella* and *Salmonella* may have selected different strategies to cope with xenophagy: while *Shigella* infection results in profound and sustained AA starvation and mTOR inhibition (see Figures 1, 2, and 3), this pathogen appears to partially escape ongoing autophagy using a disguising strategy dependent on IcsB (Ogawa et al., 2005). In contrast, *Salmonella* is shown here to act by releasing the tension (the AA starvation) on autophagy-promoting signals. At this stage, it remains unclear whether the AA starvation response in *Salmonella*-infected cells is transient because host membranes are only damaged at early times of infection (1–2 hr p.i.), or because the bacterium has developed strategies to disarm membrane damage sensing systems at later times of infection (3–4 hr p.i.). Finally, whether other vacuole-confined bacteria, such as *Mycobacterium tuberculosis*, also manipulate mTOR signaling to escape autophagy remains to be determined. In this regard, it is interesting to notice that efficient clearance of *Mycobacterium* by autophagy requires rapamycin stimulation (Gutierrez et al., 2004).

The modulation of mTOR signaling by *Salmonella* identified here is complex. In the early phase of infection (1–2 hr p.i.), two antagonistic events take place: while transient AA starvation favors a progressive detachment of mTORC1 from endomembranes, AKT activation by SopB is responsible for sustaining (and even increasing) Rheb-dependent phosphorylation of S6K1. During the AA replenishment phase (3–4 hr p.i.), our results showed that functional membrane-associated mTOR complexes dramatically accumulate at the surface of SCVs, rather than late endosomes, because at this stage the Rag GTPases (and most likely the Ragulator) seem to have been hijacked in large majority toward the maturing SCV, similarly to other late endosomal proteins. However, the reason for which 4EBP1 remains mostly dephosphorylated in *Salmonella*-infected cells remains unclear, and solving this question will likely require determining the fine nature of the mTOR complex that is formed at the surface of the SCV. Alternatively, an undefined *Salmonella* effector could be responsible for the specific dephosphorylation of 4EBP1.

Our data demonstrate that host membrane damage serves as an upstream signal that triggers and coordinates the host xenophagy defense pathway. Indeed, membrane damage response simultaneously removes the brake on autophagy by triggering AA starvation and inhibition of mTOR, while favoring peribacterial accumulation of proteins, such as NDP52, which link membrane damage with the recruitment of the autophagy machinery (Figure S6). This coordinated induction likely acts as a security system, to ensure that ramping up autophagy as a defense mechanism in bacteria-infected cells would not result in the degradation of cellular content, such as intracellular organelles. Finally, it must be pointed out that membrane damage has also been proposed to serve as a critical upstream signal for the induction of the NLRP3 inflammasome (Halle et al., 2008; Hornung et al., 2008), which plays key roles in innate immunity by triggering activation of caspase-1 and the maturation of the proinflammatory cytokines IL-1β and IL-18. Whether the existence of a common trigger (i.e., membrane damage) contributes to explain the previously identified link between autophagy and IL-1β (Saitoh et al., 2008; Zhou et al., 2011) induction remains to be identified.

In summary, we have uncovered the critical role played by AA starvation and mTOR signaling modulation in the host response to intracellular bacteria (Figure S6). By comparing the host responses to *Shigella* and *Salmonella*, two well-adapted intracellular bacterial pathogens, we also provide evidence that monitoring the dynamic changes in intracellular AA pools and mTOR signaling is key to our understanding of the multiple aspects of the host-bacterial interaction. More generally, our results highlight the importance of host metabolic perturbations in infected cells, and suggest that, in addition to autophagy, bacterial infection likely affects numerous processes regulated by AA starvation-dependent pathways, such as cell growth, proliferation and mRNA translation. These results will contribute to the development of therapeutic strategies against intracellular bacterial pathogens.

EXPERIMENTAL PROCEDURES

Antibodies and Reagents

Mouse anti-LAMP2 (ab25631), anti-GCN2 (ab70214), Rabbit anti-Phospho-GCN2 (ab75836), and Rabbit anti-NDP52 (ab68588) were from Abcam; mouse

(F) Top: HeLa cells transduced with lentiviral particles targeting a scramble sequence (Scr), RagB, RagC, or Ragulator p18 left uninfected or infected with *Salmonella* for 4 hr, analyzed by blotting with the antibodies indicated. Bottom: Protein loading adjusted to normalize for equal amounts of S6K1, and samples reanalyzed by blotting as above.
See also Figure S4.

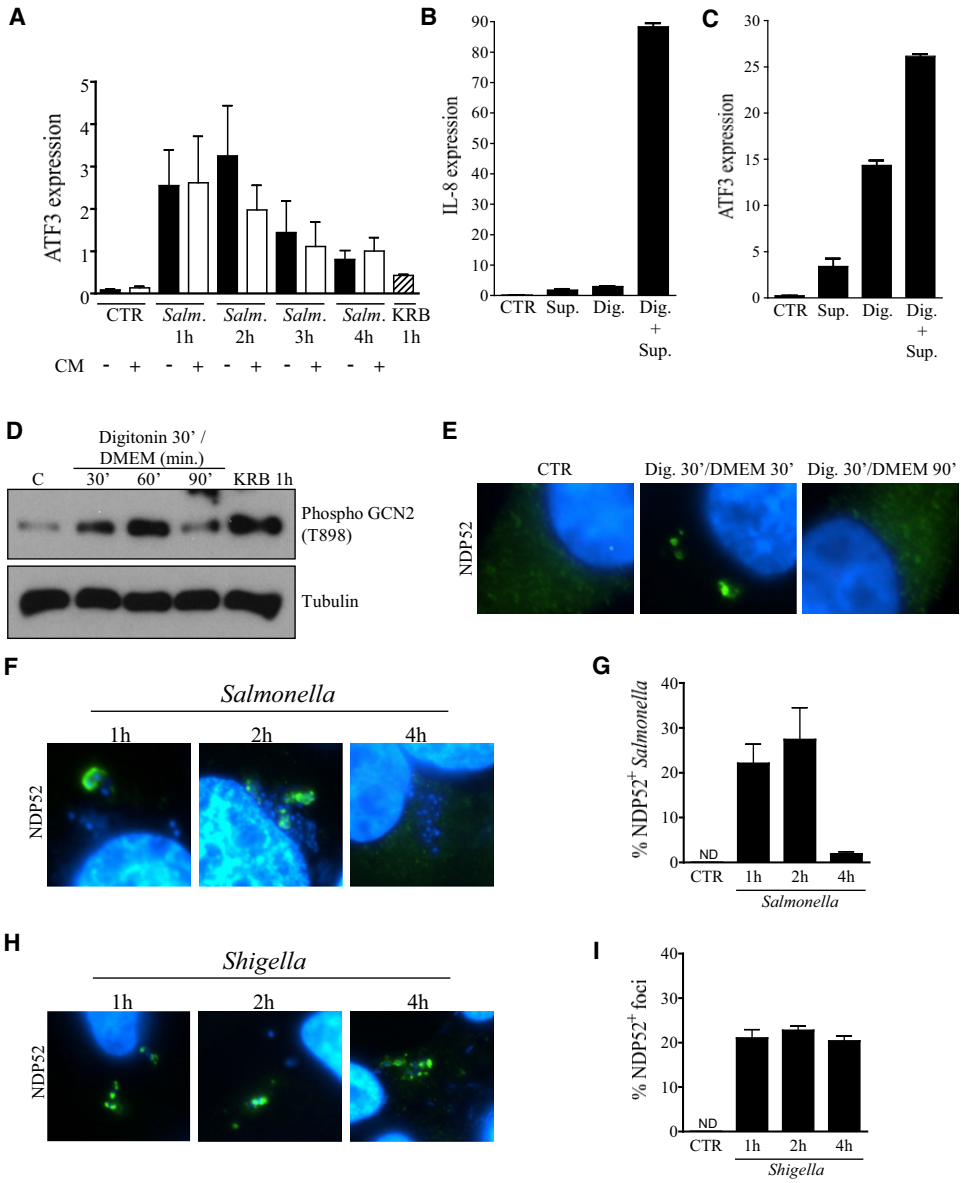

Figure 6. Membrane Damage Causes Intracellular AA Starvation

(A) HeLa cells were infected with *Salmonella* for 1 to 4 hr, in the presence or absence of 200 μg/ml chloramphenicol (CM), or were placed in AA-starvation buffer (KRB) for 1 hr, and the expression of ATF3 was determined by qPCR. Values are means + SEM. n = 3.

(B and C) HeLa cells were permeabilized with 10 μg/ml digitonin in the presence or absence of bacterial supernatant for 30 min followed by 60 min recovery in DMEM, and expression of IL-8 (B) and ATF3 (C) was determined by qPCR. Values are means + SEM of triplicate measures from one representative from three independent experiments.

(D) HeLa cells permeabilized with 10 μg/ml digitonin for 30 min followed by 30, 60, or 90 min recovery in DMEM or incubated in KRB for 1 hr as a positive control, analyzed by western blotting with anti-Phospho GCN2 (T898) and anti-tubulin antibodies.

(E) HeLa cells permeabilized with 10 μg/ml digitonin for 30 min followed by 30 or 90 min recovery in DMEM, analyzed by IF with anti-NDP52 antibody, while host nuclei are visualized with DAPI.

(F and H) HeLa cells infected with *Salmonella* (F) or *Shigella* (H) for 1, 2, or 4 hr analyzed by IF with an antibody against NDP52.

(G and I) Percentage of cell infected with *Salmonella* (G) or *Shigella* (I) displaying NDP52-positive membrane staining as observed in IF. Values are means + SEM. n = 3. ND, not detected.

See also Figure S5.

anti-tubulin clone DM1A (T9026), Sigma; rabbit anti-ATG16L1, Novus Biologicals; mouse anti-Myc (G019), Applied Biological Materials; rabbit anti-Phospho-mTOR (Ser2448) (#2971), rabbit anti-mTOR (#2983), rabbit anti-Phospho-p70S6 Kinase (Thr389) (#92345), rabbit anti-S6K1 (#9202), rabbit anti-Phospho-4EBPI (Thr37/46) (#2855), rabbit anti-4EBP1 (#9452), rabbit anti-phospho AKT substrate (#9414), rabbit anti-AKT (#9272), rabbit anti-Phospho-AKT (Ser473) (#9271), rabbit anti-Myc (#2278), and rabbit anti-RagC (#3360), Cell Signaling Technology; mouse anti-Raptor, Millipore; rabbit

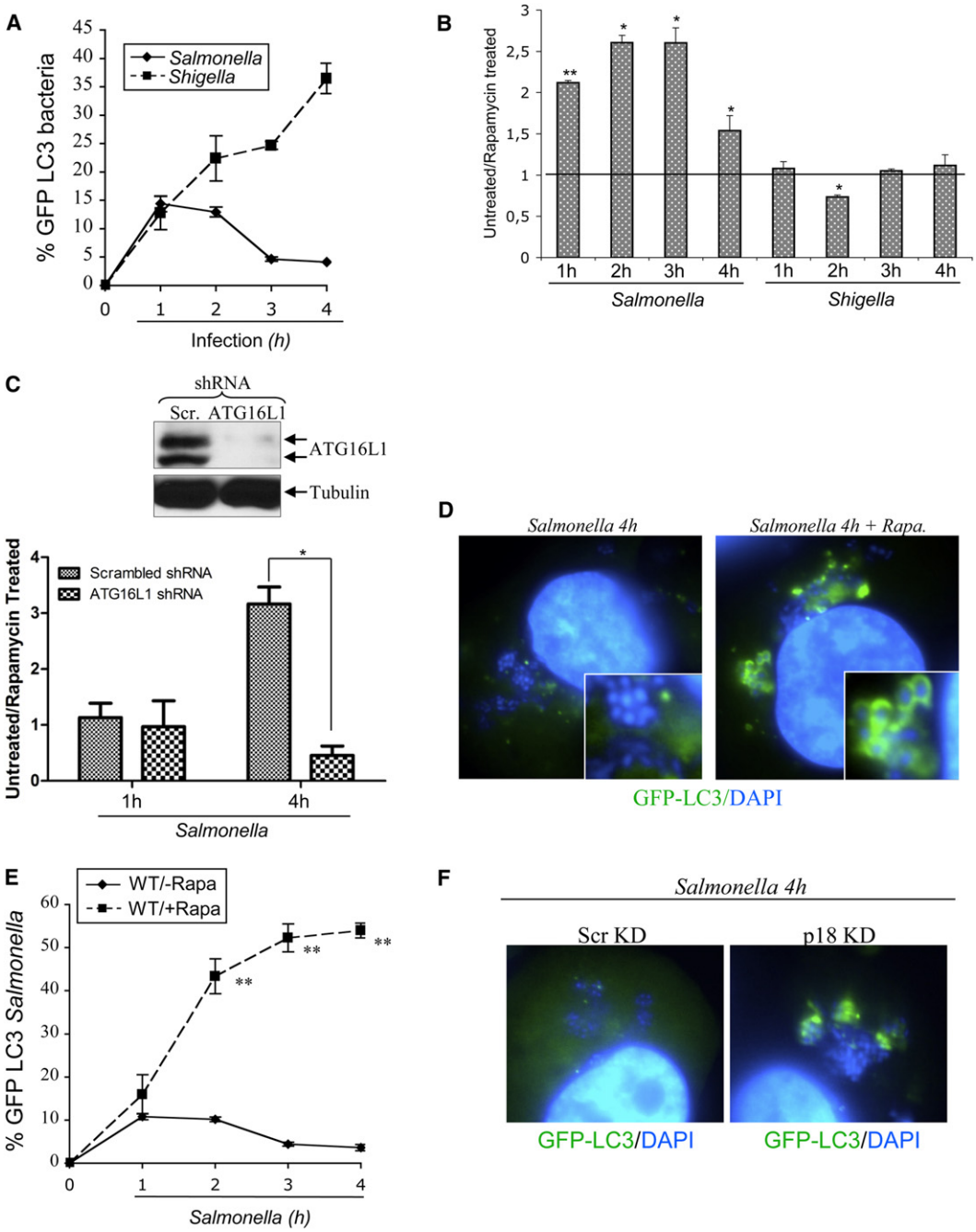

Figure 7. Pathogenic Reactivation of mTOR by *Salmonella* Results in Escape from Autophagy

(A) MDAMC cells stably expressing GFP-LC3, infected with *Shigella* or *Salmonella* for 1 to 4 hr, and the percentage of GFP-LC3+ over total intracellular bacteria determined by quantification of fluorescence microscopy analyses. Values are means ± SEM of triplicates. n = 3.

(B) HeLa cells were infected with *Shigella* or *Salmonella* for 1 to 4 hr, in the presence or absence of rapamycin, and colony-forming units (CFU) determined. Values are means + SEM of triplicates. n = 3. **$p < 0.01$ and *$p < 0.05$ for untreated over rapamycin-treated at each time point.

(C) HeLa cells transduced for 3 days with lentiviral particles targeting a scramble sequence or ATG16L1, analyzed by blotting using the antibodies indicated (top) to evaluate ATG16L1 expression knockdown, or infected with *Salmonella* for 1 to 4 hr, and CFU determined (bottom). Values are means + SEM of triplicates. n = 3. *$p < 0.05$.

(D) MDAMC cells stably expressing GFP-LC3, infected with *Salmonella* for 4 hr in the presence or absence of rapamycin, analyzed by fluorescence microscopy.

(E) Percentage of GFP-LC3+ over total intracellular bacteria was determined at different time points. Values are means ± SEM of triplicates. n = 3. **$p < 0.01$ over non-rapamycin stimulated.

(F) MDAMC cells stably expressing GFP-LC3, transduced for 3 days with lentiviral constructs targeting either a Scramble (Scr) sequence or Ragulator p18 were infected with *Salmonella* for 4 hr and analyzed by fluorescence microscopy.

See also Figure S6.

anti-Tia-1, Santa Cruz Biotechnology; Goat anti-rabbit IgG and Goat anti-mouse IgG peroxidase conjugated, Thermo Scientific; and FITC-conjugated Goat anti-rabbit and Cy3-conjugated Goat anti-mouse, Jackson ImmunoResearch Laboratories. Rapamycin (50 μg/ml) was from LKT Laboratories; AKT inhibitor IV, Santa Cruz Biotechnology; 4′,6-diamidino-2-phenylindole (DAPI), Vector Laboratories; Chloramphenicol (C-0857), digitonin (D141), Sigma; and L-glutamine, GIBCO Invitrogen. Glycyl-L-phenylalanine 2-naphthylamide (GPN) was from Santa Cruz Biotechnology.

Bacterial Strains and Cell Culture

Invasive (M90T) strain of *Shigella flexneri* was grown in Tryptic Soy Broth (Becton Dickinson). *Salmonella Typhimurium* SL1344 was grown in Luria-Bertani broth (Invitrogen by Life Technology). The SopB– *Salmonella* strain was provided by Dr. Brumell (HSC, Toronto, Canada). Human breast carcinoma epithelial cells (MDAMC cells) stably transfected with GFP-LC3 were from Dr. Yoshimori (Osaka University). The human epithelial HeLa cell line (American Type Culture Collection), MDAMC cells, mouse embryonic fibroblasts from WT mice, and mice expressing eIF2α S51A (a gift from Dr. Kaufman, University of Michigan), were cultured in Dulbecco's modified Eagle medium (DMEM) supplemented with 10% fetal calf serum (FCS), 2 mM L-glutamine, 50 IU penicillin, and 50 μg/ml streptomycin. Cells were maintained in 95% air, 5% CO_2 at 37°C. Endotoxin-free FCS and phosphate-buffered saline (PBS) were from Wisent (Saint-Bruno-de-Montarville, Quebec, Canada).

Bacterial Infection

Overnight bacterial cultures of *Shigella* or *Salmonella* were diluted 100-fold and grown to exponential phase (OD_{600} = 0.4 to 0.6) in aerobic conditions, collected by centrifugation 5,000 g for 5 min, washed in saline buffer (150 mM NaCl) and resuspended in DMEM. Cells cultured in antibiotic-free medium were infected at a multiplicity of infectionof 100, centrifuged (2,000 g for 15 min at 37°C), and incubated at 37°C/5% CO_2 for 15 min. Cells were washed three times with PBS and fresh medium containing gentamicin (50 μg/ml) added. For gentamycin-protection assays, infected cells were washed three times with PBS and then lysed with 0.1% Triton X-100 in PBS. Lysates were plated on LB agar in 10-fold dilutions, and colonies were enumerated on the following day. Where indicated, rapamycin was added to the cells 1 hr prior to infection and with the gentamycin-containing media. For the preparation of bacterial supernatants in digitonin experiments, overnight culture of *Shigella* was centrifuged and filtered (0.22 μm), and used at a 1/100 dilution.

Buffer for Amino Acid Starvation

Cells rinsed three times with PBS were incubated in Krebs Ringer Bicarbonate (KRB) buffer (118.5 mM NaCl, 4.74 mM KCl, 1.18 mM KH2PO4, 23.4 mM NaHCO3, 5 mM glucose, 2.5 mM CaCl2, and 1.18 mM MgSO4, adjusted to pH 7.6 by titration with 1 N NaOH).

Immunofluorescence Microscopy

HeLa cells placed on glass coverslips were processed for IF as previously described (Travassos et al., 2010). Samples were visualized on a Carlo Zeiss Axiovert 200 microscope with a 63× oil fluorescence objective, and images were analyzed with Volocity software (Quorum Technologies). Nuclei and bacteria were visualized with DAPI staining.

Western Blotting

Cells were washed twice in cold PBS, lysed in ice-cold lysis buffer: 40 mM HEPES (pH 7.4), 120 mM NaCL, 1 mM EDTA, 0.3% CHAPS, EDTA-free protease inhibitors, and Phosphatase inhibitor cocktail (Roche). Soluble fractions of lysates were isolated by centrifugation at 12,000 rpm for 10 min at 4°C. Protein concentration was determined with Bradford (Pierce).

shRNA Lentivirus Packaging and Transduction

shRNA sequences were inserted into the pLKO.1 vector (Addgene). Packaging and purification of shRNA-expressing lentivirus, with the lentiviral packaging/envelope vectors psPAX2 and pMD2.G, were performed according to procedures previously described (Benko et al., 2010), with few adjustments: cells were systematically analyzed 3–4 days after lentiviral transduction, and neomycin selection was omitted. The following sequences were used: hRheb1 (5′-CCTCAGACATACTCCATAGAT-3′), hRagC (5′-TGGCAATTATCAAGCTGAATA-3′), hRagB (5′-CGGGACAACATCTTCCGAAAT-3′), hp18 (5′-AGACAGCCAGCAACATCATTG-3′), hRaptor (5′-GGCTAGTCTGTTTCGAAATTT-3′), hRictor (5′-GCAGCCTTGAACTGTTTAA-3′), and hATG16L1 (5′-GCATGAATGTGTCTCATTACT-3′).

Expression Vectors and Transfection

Expression vectors encoding for HA-tagged chimeric protein of Raptor fused to 15 amino acids of Rheb (Rheb-Rap) and HA-RagB 99L were from Addgene. Transfection was performed with Fugene (Roche) according to the manufacturer's instructions.

Measurement of Cytosolic L-Leucine/L-Isoleucine Levels

Cell pellets were washed with 3 volumes of isotonic ice-cold buffer. Cellular lysates were prepared using freeze-thawing and methanol/water extraction. The resulting cellular lysates were evaporated, redissolved in 200 μl water/acetonitrile (9/1, v/v) containing 200 ng/ml leucine-d3 internal standard (C/D/N Isotopes). After centrifugation (10 min, 14000 rpm, 4°C), 20 μl of each sample was injected in duplicate for LC-MS/MS analysis. LC-MS/MS system consisted of refrigerated CTC Pal autosampler, Thermo MS Surveyor pumps and Thermo TSQ Vantage triple-quadrupole MS instrument equipped with HESI probe. LC separation was performed with Hypercarb column (100 × 2.1 mm, 5 μm particle size), and gradient elution with acetonitrile/water/formic acid was used at 300 μl/min flow rate. MS analysis was performed with selected reaction monitoring mode: 132.1→86.1 (leucine and isoleucine) and 135.1→89.1 (leucine-d3). Transitions 132.1→41.0 and 132.1→69.0 were used for confirmation purposes. Leucine and isoleucine were not chromatographically resolved; therefore, the amounts are reported as total of leucine and isoleucine after calibration using nine-standard calibration curve (50–3,000 ng/ml) and the correction for 5-fold preconcentration of samples. The efficiency of removal of extracellular AA with the above washing procedure prior to cell lysis was verified by ensuring that no AA were detected in the final wash with the same LC-MS/MS analysis.

Quantification of Events Observed in IF

The percentage of cells displaying colocalization of mTOR on LAMP2+ vesicles, Tia-1+ stress granules, and the percentage of bacteria targeted by GFP-LC3 was analyzed by IF. For each analysis, at least 100 cells from randomly selected fields were counted for each time point and condition, in at least three independent experiments. Results are expressed as means ± SEM of data obtained in these independent experiments.

Microarray Analysis

Total RNA from HeLa cells left unstimulated, stimulated with rapamycin, or infected with *Shigella* for 4 hr was used to probe Affymetrix microchips (GeneChip Human Exon 1.0 ST). For each condition, three independent biological replicates were tested, each on distinct microchip, and were analyzed with Affymetrix software. For each gene, fold induction over control condition was calculated, and genes were further ranked based on relative fold induction.

Quantitative PCR

Real-time PCR analysis of *ATF3*, *CHOP*, *CHAC1*, and *IL-8* expression was performed with SYBR green reagents, and normalized to the endogenous housekeeping control, *β-actin*, as previously described (Benko et al., 2010).

Statistical Analysis

Significant differences between mean values were evaluated with a one-sample or unpaired t tests.

ACCESSION NUMBERS

The accession number for the microarray analysis presented in Figure 2 is GSE38055.

SUPPLEMENTAL INFORMATION

Supplemental Information includes six figures and can be found with this article online at doi:10.1016/j.chom.2012.04.012.

ACKNOWLEDGMENTS

This work was supported by grants from the Burroughs Wellcome Fund (to S.E.G.) and the CIHR (to D.J.P.). We thank Mauricio Terebiznik (University of Toronto at Scarborough), Kaoru Geddes, and William W. Navarre (University of Toronto) for helpful discussions.

Received: May 20, 2011
Revised: March 19, 2012
Accepted: April 10, 2012
Published: June 13, 2012

REFERENCES

Avruch, J., Long, X., Ortiz-Vega, S., Rapley, J., Papageorgiou, A., and Dai, N. (2009). Amino acid regulation of TOR complex 1. Am. J. Physiol. Endocrinol. Metab. *296*, E592–E602.

Benko, S., Magalhaes, J.G., Philpott, D.J., and Girardin, S.E. (2010). NLRC5 limits the activation of inflammatory pathways. J. Immunol. *185*, 1681–1691.

Birmingham, C.L., Smith, A.C., Bakowski, M.A., Yoshimori, T., and Brumell, J.H. (2006). Autophagy controls Salmonella infection in response to damage to the Salmonella-containing vacuole. J. Biol. Chem. *281*, 11374–11383.

Brumell, J.H., and Grinstein, S. (2004). Salmonella redirects phagosomal maturation. Curr. Opin. Microbiol. *7*, 78–84.

Cemma, M., Kim, P.K., and Brumell, J.H. (2011). The ubiquitin-binding adaptor proteins p62/SQSTM1 and NDP52 are recruited independently to bacteria-associated microdomains to target Salmonella to the autophagy pathway. Autophagy *7*, 341–345.

Cooney, R., Baker, J., Brain, O., Danis, B., Pichulik, T., Allan, P., Ferguson, D.J., Campbell, B.J., Jewell, D., and Simmons, A. (2010). NOD2 stimulation induces autophagy in dendritic cells influencing bacterial handling and antigen presentation. Nat. Med. *16*, 90–97.

Girardin, S.E., Boneca, I.G., Carneiro, L.A., Antignac, A., Jéhanno, M., Viala, J., Tedin, K., Taha, M.K., Labigne, A., Zähringer, U., et al. (2003). Nod1 detects a unique muropeptide from gram-negative bacterial peptidoglycan. Science *300*, 1584–1587.

Gutierrez, M.G., Master, S.S., Singh, S.B., Taylor, G.A., Colombo, M.I., and Deretic, V. (2004). Autophagy is a defense mechanism inhibiting BCG and Mycobacterium tuberculosis survival in infected macrophages. Cell *119*, 753–766.

Halle, A., Hornung, V., Petzold, G.C., Stewart, C.R., Monks, B.G., Reinheckel, T., Fitzgerald, K.A., Latz, E., Moore, K.J., and Golenbock, D.T. (2008). The NALP3 inflammasome is involved in the innate immune response to amyloid-beta. Nat. Immunol. *9*, 857–865.

Hornung, V., Bauernfeind, F., Halle, A., Samstad, E.O., Kono, H., Rock, K.L., Fitzgerald, K.A., and Latz, E. (2008). Silica crystals and aluminum salts activate the NALP3 inflammasome through phagosomal destabilization. Nat. Immunol. *9*, 847–856.

Huang, J., and Manning, B.D. (2009). A complex interplay between Akt, TSC2 and the two mTOR complexes. Biochem. Soc. Trans. *37*, 217–222.

Jiang, H.Y., Wek, S.A., McGrath, B.C., Lu, D., Hai, T., Harding, H.P., Wang, X., Ron, D., Cavener, D.R., and Wek, R.C. (2004). Activating transcription factor 3 is integral to the eukaryotic initiation factor 2 kinase stress response. Mol. Cell. Biol. *24*, 1365–1377.

Klionsky, D.J. (2007). Autophagy: from phenomenology to molecular understanding in less than a decade. Nat. Rev. Mol. Cell Biol. *8*, 931–937.

Levine, B., Mizushima, N., and Virgin, H.W. (2011). Autophagy in immunity and inflammation. Nature *469*, 323–335.

Ogawa, M., Yoshimori, T., Suzuki, T., Sagara, H., Mizushima, N., and Sasakawa, C. (2005). Escape of intracellular Shigella from autophagy. Science *307*, 727–731.

Ramsden, A.E., Holden, D.W., and Mota, L.J. (2007). Membrane dynamics and spatial distribution of Salmonella-containing vacuoles. Trends Microbiol. *15*, 516–524.

Saitoh, T., Fujita, N., Jang, M.H., Uematsu, S., Yang, B.G., Satoh, T., Omori, H., Noda, T., Yamamoto, N., Komatsu, M., et al. (2008). Loss of the autophagy protein Atg16L1 enhances endotoxin-induced IL-1beta production. Nature *456*, 264–268.

Sancak, Y., Peterson, T.R., Shaul, Y.D., Lindquist, R.A., Thoreen, C.C., Bar-Peled, L., and Sabatini, D.M. (2008). The Rag GTPases bind raptor and mediate amino acid signaling to mTORC1. Science *320*, 1496–1501.

Sancak, Y., Bar-Peled, L., Zoncu, R., Markhard, A.L., Nada, S., and Sabatini, D.M. (2010). Ragulator-Rag complex targets mTORC1 to the lysosomal surface and is necessary for its activation by amino acids. Cell *141*, 290–303.

Sengupta, S., Peterson, T.R., and Sabatini, D.M. (2010). Regulation of the mTOR complex 1 pathway by nutrients, growth factors, and stress. Mol. Cell *40*, 310–322.

Steele-Mortimer, O., Knodler, L.A., Marcus, S.L., Scheid, M.P., Goh, B., Pfeifer, C.G., Duronio, V., and Finlay, B.B. (2000). Activation of Akt/protein kinase B in epithelial cells by the Salmonella typhimurium effector sigD. J. Biol. Chem. *275*, 37718–37724.

Thurston, T.L., Ryzhakov, G., Bloor, S., von Muhlinen, N., and Randow, F. (2009). The TBK1 adaptor and autophagy receptor NDP52 restricts the proliferation of ubiquitin-coated bacteria. Nat. Immunol. *10*, 1215–1221.

Thurston, T.L., Wandel, M.P., von Muhlinen, N., Foeglein, A., and Randow, F. (2012). Galectin 8 targets damaged vesicles for autophagy to defend cells against bacterial invasion. Nature *482*, 414–418.

Travassos, L.H., Carneiro, L.A., Ramjeet, M., Hussey, S., Kim, Y.G., Magalhães, J.G., Yuan, L., Soares, F., Chea, E., Le Bourhis, L., et al. (2010). Nod1 and Nod2 direct autophagy by recruiting ATG16L1 to the plasma membrane at the site of bacterial entry. Nat. Immunol. *11*, 55–62.

Wek, R.C., Jiang, H.Y., and Anthony, T.G. (2006). Coping with stress: eIF2 kinases and translational control. Biochem. Soc. Trans. *34*, 7–11.

Wullschleger, S., Loewith, R., and Hall, M.N. (2006). TOR signaling in growth and metabolism. Cell *124*, 471–484.

Xu, Y., Jagannath, C., Liu, X.D., Sharafkhaneh, A., Kolodziejska, K.E., and Eissa, N.T. (2007). Toll-like receptor 4 is a sensor for autophagy associated with innate immunity. Immunity *27*, 135–144.

Yoshikawa, Y., Ogawa, M., Hain, T., Yoshida, M., Fukumatsu, M., Kim, M., Mimuro, H., Nakagawa, I., Yanagawa, T., Ishii, T., et al. (2009). Listeria monocytogenes ActA-mediated escape from autophagic recognition. Nat. Cell Biol. *11*, 1233–1240.

Zhang, H., Zha, X., Tan, Y., Hornbeck, P.V., Mastrangelo, A.J., Alessi, D.R., Polakiewicz, R.D., and Comb, M.J. (2002). Phosphoprotein analysis using antibodies broadly reactive against phosphorylated motifs. J. Biol. Chem. *277*, 39379–39387.

Zhou, R., Yazdi, A.S., Menu, P., and Tschopp, J. (2011). A role for mitochondria in NLRP3 inflammasome activation. Nature *469*, 221–225.